Research Square

Preprints are preliminary reports that have not undergone peer review.
They should not be considered conclusive, used to inform clinical practice,
or referenced by the media as validated information.

Binding Affinities of Sanggenon Derivatives as PTP1B Inhibitors; Using Molecular Dynamics and Free Energy Calculations

Safak OZHAN KOCAKAYA (safakozhan@dicle.edu.tr)
Dicle University

Research Article

Keywords: PTP1B Inhibitors, Sanggenon, , Molecular dynamics simulation, Molecular docking Binding energy analysis, MM-PBSA analysis

Posted Date: June 7th, 2021

DOI: https://doi.org/10.21203/rs.3.rs-598375/v1

License: This work is licensed under a Creative Commons Attribution 4.0 International License.
Read Full License

Abstract

Recently, protein tyrosine phosphatase 1B (PTP1B) inhibitors have become the frontier as possible targeting for anti-cancer and antidiabetic drugs. The contemporary observe represents a pc assisted version to investigate the importance of precise residues within the binding web site of PTP1B with numerous Sanggenon derivatives remoted from nature. Molecular dynamics (MD) simulations were performed to estimate the dynamics of the complexes, and absolute binding unfastened energies have been calculated with exclusive additives, and carried out through the usage of the Molecular Mechanics-Poisson-Boltzmann floor region (MM-PB/SA) and Generalized Born surface vicinity (MM-GB/SA) strategies. The effects show that the expected free energies of the complexes are normally constant with the available experimental statistics. MM/GBSA free energy decomposition analysis shows that the residues Asp29, Arg24, Met258, and , Arg254 in the second active site in PTP1B are crucial for the excessive selectivity of the inhibitors.

Introduction

PTP1B (protein-tyrosine phosphatase 1B) is a non-transmembrane enzyme found on the endoplasmic reticulum (ER) and is a broadly expressed phosphatise. It plays a relevant modulator position in signaling pathways initiated through the activation of the tyrosine kinase receptor superfamily. [1,2]. It is thought that PTP1B is involved in a critical node of insulin signaling by dephosphorylating and inactivating the insulin receptor, thus switching off insulin signaling. PTP1B is likewise implicated in the manipulate of immune mobile signaling, controlling cytokine signaling pathways via dephosphorylation of janus kinase 2 (JAK2), non-receptor tyrosine-protein kinase 2 (TYK2) and sign transducer and activator of transcription 5 (STAT5) [3,4]. furthermore, it's far believed that interleukin-4 (IL-four) induces PTP1B mRNA in a phosphatidylinositol three-kinase (PI3K)-established manner and increases PTP1B protein stability to suppress IL-four-precipitated STAT6 signaling. The excessive affinity substrate binding by PTPs is caused by the phosphoryl group and amino acid residues flanking the phosphotyrosyl (pTyr) residue [5,6]. pTyr residues are liable to hydrolysis by cellular phosphatates and consequently they are not ideally suited for inhibitor development. consequently incorporation of non-hydrolizable phosphate mimetics inclusive of phosphonemethylphenylalanine (pmp), phosphonodiflouromethylphenylalanine (F2pmp), into a selected gold standard peptide template were employed in the development of mighty and selective PTP1B inhibitors [7]. even though those peptide inhibitors are most effective, aggressive and selective PTP1B inhibitors, difficulties in their cellular membrane shipping and the reality that they are peptide phosphonates cause them to less proper as drug applicants [8,9].

Although there are a number of reports on the designing and development of synthetic PTP1B inhibitors, only a few studies cover PTP1B inhibitors derived from plants. Rollinger et al. reported Sanggenon molecules, as antifungal compounds, and isolated them from Methanol Morus root bark extract by bio-guided fractionation [10].

It has recently been reported that Sanggenon derivatives, which has showed antifungal activities, also possess inhibition effects on PTP1B. The present paper aims to describe a detail of binding mode of PTP1B with Sanggenon derivatives. The reasons for choosing these molecules are that they have already got experimental IC_{50} values with PTP1B for comparison and they are good candidates because they can be easily isolated from nature and are potential scaffolds for chemical modifications to develop and design new drugs [11]. We have chosen this series to clarified their binding pose with PTP1B by docking and MD simulations and to derive structure–activity relationship. They have been employed to reveal the structural factors responsible for selectivity of inhibitors between antifungal Sanggenon compounds and human PTP1B.

The inhibition effect of the molecules was facilitated by the usage of the Molecular Mechanics-Poisson-Boltzmann Surface Area and the Generalized Born Surface Area Methods.

The complex structure of every compound was modelled through the use of the Dock 6.5 program scoring feature [12]. every complex structure become eventually subjected to a molecular dynamics (MD) simulation of 10 ns long with the aid of the usage of the AMBER 11.0 application [13,14]. primarily based on the configuration ensembles retrieved from the MD trajectories, a MM-PB/SA become employed to compute the binding free energies of all four PTP1B inhibitors. numerous elements of the MM-PB/SA method have been explored in the take a look at with the intention to acquire optimized effects. The X-score scoring function become located to produce similarly desirable effects as MM-PB/SA on each complex systems become prepared by using molecular docking, and the configurationally ensembles received thru lengthy MD simulations [15]. The molecule dynamics (MD) calculation, decomposition analysis and free energy were employed to examined the detailed binding mechanisms of the Sanggenon inhibitors based on the second active site of PTP1B [16,17] The performance of MM-PB/SA was slightly inferior to that of MM-GB/SA.

Method All molecular dynamic calculations were executed the use of the Assisted model building with energy Refinement (AMBER) suite of programs (version eleven). 3-D systems had been displayed using Chimera (UCSF [18], DSV [19]. RMSD snap shots were proven by way of the XMGRACE [20] package program. XLeAP as applied in AMBER became employed to put together parameter/topology and coordinate files and solvate and additionally to neutralize the system for the MD simulations. Systems have been solvated with a TIP3P [21] water model with the aid of growing an isometric water container where the gap of the field is 10 Å from the periphery of the protein-ligand complex. An ff99SB pressure area turned into used for the protein. Atomic partial expenses had been determined by way of the antechamber module of the AMBER package using AM1-Bcc (Austian model with Bond and charge correction) for the ligands and the overall AMBER pressure area (GAFF) [22] became adopted in simulation for the ligands as it handles small natural molecules. Hydrogen bond analyses between the protein and the ligands and RMSD adjustments with time throughout MD simulations were calculated by way of the ptraj module as applied within the AMBER applications package.

Preliminary complexes had been placed in a cubic field of express TIP3P water molecules with a maximum distance between the protein and the edge of the container of 10 Å. The essential counterions have been added in an effort to neutralize the systems. Periodic boundary conditions were used in all simulations with the Particle Mesh Ewald approach [23] to compute long electrostatic interactions. A cut off distance of 10 Å was chosen to compute Van der Waals (VdW) non-bonded interactions. 1 ns MD simulation became carried out for each ligand in a vacuum, at three hundred ok. Each complex shape became then subjected to a molecular dynamics (MD) simulation of 10 ns lengthy the use of the AMBER v11 software. Primarily based on the configurational ensembles revoked from the MD trajectories, MM-PB/SA became employed to compute the binding unfastened energies of all 4 PTP1B inhibitors. The performance of MM-PB/SA became barely not so good as that of MM-GB/SA. Several factors of the MM-GB(PB)/SA method had been explored in this observe to reap optimized consequences. The molecule dynamics (MD) simulation, unfastened strength calculations and free strength decomposition analysis had been hired to analyze the detailed binding mode of the Sanggenon derivative inhibitors based on the second binding site of PTP1B. All inhibitor structures are proven in (Figure1).

1.1 Molecular Docking

Dock 6.5 module permits the appearing of all tiers of a docking technique, era of ligand conformations, ligand docking, and scoring of the binding modes. As in this example, in which a inflexible receptor approximation turned into used, it is expected that the special receptors taken into consideration will lead to distinct ligand-binding modes depending on the preliminary size of the PTP1B-binding cavity. For this reason, the four new PTP1B inhibitors had been docked into the available the receptor binding following a multistep process. On the way to describe receptor-binding site, a grid of potential energy changed into calculated for atoms inside the binding pocket. These atoms had been obtained from the analysis of each protein–ligand complex. In this step, default parameters had been used. Then, the ligand changed into docked the usage of the calculated grid to vicinity it into the cavity and rating the proposed binding modes.

2.2 Molecular Dynamics Simulations

The initial enzyme structure of PTP1B was obtained from the Protein Data Bank of Brokhaven National Laboratory (PDB entry 1wax) [24]. 1wax.pdb has 2.20 Å resolution and already has an inhibitors in its structure for comparison of docking. 1wax.pdb sequence has shown Figure 8. Crystallographic water molecules had been removed from all of the structures and the missing coordinates of the atoms had been modelled the use of xLeAP and an ff99SB force subject. Atoms on PTP1B had been assigned the PARM99 expenses, and all ionizable residues were set at their default protonation states at impartial pH. All systems had been similarly processed by way of the xLeAP module of AMBER. Structures have been solvated with a TIP3P water model through growing an isometric water container, in which the space of the box is 10 Å from the periphery of protein. The molecular systems had been neutralized through the addition of counterions. The systems have been minimized in two steps; inside the first step, the protein and ligand had been saved constant, most effective the water molecules had been allowed to move, and

within the 2d step, all atoms had been allowed to move. For step one, the energy minimization became performed in 500 and 2500 steps with the steepest descent and conjugate gradient methods, respectively. For the second step, the strength minimizations have been done in 500 and 2500 steps the use of the steepest descent and conjugant gradient techniques, respectively. Heating changed into done with an NVT ensemble for two hundred playstation where the protein-ligand complex turned into limited with a force consistent of 10 kcal/mol/Å. Equilibration was achieved for two hundred playstation on an NPT ensemble restraining the protein-ligand complicated with the aid of 1 kcal/mol/Å2. Final simulations, the production phase, had been done for five ns on an NPT ensemble at a 300 okay temperature and 1 atm strain without any restrain. Step length changed into 2 fs for the complete simulation. A Langevin thermostat and barostat have been used for coupling the temperature and pressure. A SHAKE algorithm become implemented to constrain all bonds containing hydrogen atoms. The nonbonded cut off turned into stored at 10 Å, and lengthy range electrostatic interactions had been treated by using the particle mesh Ewald (PME) approach with a fast Fourier rework grid with approximately zero.1 nm area. Trajectory snapshots, which had been eventually used for evaluation, had been taken at each 1 ps. [25]

2.3 MM-PB/SA

The MM-PBSA (molecular mechanics Poisson–Boltzmann surface location) technique is held to be one of the greater computationally tractable approach of acquiring affordable estimates of the free energy of a complicated device. In essence, it is quite trustworthy: one performs a conventional molecular dynamics simulation of the complex in a periodic water box with counterions and the resulting trajectory is then publish-processed with the aid of removing the solvent and the periodicity and calculating the average of loose electricity over a series of static frames or “snapshots” consistent with the formula below.

$$G = E_{MM} + G_{polar} + G_{nonpolar} - TS_{MM}$$

Here, EMM is the average sum of molecular mechanical strength terms, Ebond + Eangle + Etorsion + EVdW + Eelectrostatic Gpolar and Gnonpolar describe the unfastened power of the solvent continuum. The Gpolar time period can be obtained both thru the answer of the Poisson–Boltzmann equation, or the use of an equal Generalized Born approximation. The Gnonpolar part is typically acquired by means of scaling the solvent available floor region with the aid of the appropriate surface anxiety. S is the entropy of the solute either from quasi-harmonic evaluation of the trajectory or from normal mode calculations on a (restrained) range of snapshots. Then binding free energies are acquired from

$$\Delta G_{binding} = G_{complex} - G_{receptor} - G_{ligand}$$

All energy additives have been calculated the use of a 100 snapshots from 1 ns to 5 ns. The snapshots from 1 to 5 ns molecular dynamics (MD) simulation trajectories were taken from the calculation of free energy. For PBSA and GBSA calculations, dielectric constants solvent became taken as 80.0, respectively.

2.4 Free Energy Decomposition Analysis

Free energy turned into decomposed to estimate the contribution of every residue in the binding procedure and was completed the use of MM/PBSA. The free energy turned into calculated by using the MM/GBSA method. The energy of every residue-inhibitor interaction is given by using the subsequent equation:

$$\Delta G_{inhibitor\text{-}residue} = \Delta E_{vdw} + \Delta E_{ele} + \Delta G_{GB} + \Delta G_{SA} \quad (5)$$

Where in ΔG_{GB} is free energy due to the solvation process of polar contribution calculated using the generalized Born model. MD simulation trajectories in the 5 ns were taken, and all energies were calculated for each frame. Total energy, the average energy of backbone and side chains for each residue was calculated. In order to get the contribution of each residue to the total binding energy.

Where ΔG_{GB} is free energy due to the solvation process of polar contribution calculated using the generalized Born model, ΔG_{SA} is free energy due to a surface area factor. MD simulation trajectories at the range of 1- 5 ns were taken, and all the energies were calculated for each frame. The average energy of backbone and side chains for each residue was separately calculated, and the total energy was calculated as well [26].

Results And Discussion

The structures of Sanggenon derivatives used in this study are presented in Figure 1. The lowest energy conformers for each derivative were located by performing simulated annealing. These conformers were used for docking. All the ligands were selectively docked into the active site of the enzyme. They produce docking scores ranging from -47 to -60 kcal mol^{-1} as shown in Table 1.

Table 1. Calculated thermodynamic parameters for complexation of Sanggenon derivatives

by docking method.

inhibitors	*ΔE_{vdw}	*ΔE_{ele}	*Dock score
1	-37.33	-9.80	-47.14
2	-49.35	-11.10	-60.45
3	-50.53	-9.44	-59.97
4	-45.02	-11.13	-56.15

*kcal mol^{-1}

Before docking these derivatives, the molecule in the x-ray structure was docked into the protein and it was found that all the ligands are docked into the same location of this molecule as shown in Figure 2.

Each complex was subjected to MD calculations for a period of 10 ns. To explore the dynamic stability of these four protein/inhibitor complexes, and to ensure the rationality sampling strategy, root-mean-square deviations (RMSD) values of the protein were plotted in Figure 3.

The RMSD plots show that the conformations of the complexes usually achieve equilibrium at ~300 ps, while with some conformations; this equilibrium time is ~600 ps. A Kinetic energy, potential energy and total energy of PTP1B complexes are represented in Figure 4.

Trajectory data from MD trajectories were analyzed in terms of hydrogen bonding interactions, orientation of the inhibitor within the active site, other interactions such as aromatic p–p stacking and hydrophobic interactions, RMS deviation of the active site residues and binding energy (Figure 5).

To compare the orientation of the ligands in the active site of the protein, all compounds were superimposed, as indicated in Figure 6. They illustrated that all the compounds showed similar interaction modes of binding in the second active site of PTP1B. Orientation of these inhibitors in the enzyme B site indicates that the interaction of the hydrogen bond is of great importance during binding (Deora et al., 2013; Puius et al., 1997).

The presence of the occupancy between compound 1- 4 and residue bonds is summarized in Table 3. The role of Gln102 and Asp29 residues in particular are notable in the hydrogen bond formation for the complex of the protein with the ligands as shown in Table 3. Additionally, other residues play key roles in the interaction of the enzyme with Sanggenon derivatives. These are Arg24 and Arg254 via hydrogen bonds, Met258 via van der Waals interactions and Phe182 via pi-pi interaction Figure 6. The two dimensional docking diagram is shown in Figure 7 the effect of amino acids on it can be seen more clearly.

The RMSF fluctuations for the complexes of PTP1B with inhibitors showed that the residues in the active site of binding are more intact, indicating the tight binding of the inhibitors (Fig. 8). The decomposition energy values are also consistent with the RMSF. Overall, the structures with the same proteins share similar RMSF distributions and similar trends of dynamic features.

The efficiency of a ligand binding to a protein can be estimated by the snapshots from a trajectory of the complex in the MM/PBSA calculations. The binding free energies and the energy components of the complexes are shown in Table 2. It was gratifying that the available experimental data of the inhibitors (IC_{50}) are consistent with the molecular model results as noted in Table 2. It indicates that **3** (IC_{50}=1.6 μM) has a larger energy of binding compared with **2** (IC_{50}=2.6 μM). The available data was compared to the correlations between the available experimental IC_{50} and each of the five free energy components, ΔE_{ele}, ΔE_{vdw}, ΔG_{PB}, ΔG_{GB}, ΔH and calculated K_i. The calculated data demonstrated that the polar contribution, electrostatic interaction and the polar part of the desolvation and hydrogen bonds enhance the binding of the inhibitors. The results indicate that the electrostatic componets (ΔE_{ele}+ΔG_{PB}) contibute more to the binding energy compared with the non-polar (ΔE_{vdw}+ΔG_{SA}) components. The free energy of

the complexations is observed in the range of -7.37 to -13.16 kcal/mol, respectively. Orientation of these inhibitors in the enzyme B site indicates that the interaction of the hydrogen bond is of great importance during binding. The role of Gln102 and Asp29 residues in particular are notable in the hydrogen bond formation for the complex of the protein with the ligands as shown in Table 3. The presence of the occupancy between compound 1- 4 and residue bonds is summarized in Table 3. The result shows that compound 2 and compound 4 with a similar chemical structure but with different stereochemistry are effective on inhibition. Furthermore, compound 1 has the highest activity among the natural Sanggenon derivatives, which can be interpreted from its high interaction energy. Having a high total enclosed volume, compound 1 effectively occupied the van der Waals contacts of Met258. Additional hydrogen bonds and electrostatic interactions, with the residues of the Asp29, Arg254, Arg24 contributed significantly toward the enhanced inhibitor activity of compound 1. Moreover, compound 1 and 2, compounds 1, 2 exhibit similar activity and interactions, and Van der Waals with Met258, Asp29 and the electrostatic contacts of the inhibitors with the Arg24, Arg254, as illustrated in Figure 1, generally belong to the same category. The three dimensional projection of the complexes in Figure 6, point to the connection areas of the ligands and the locations of the connection area. The most effective amino acids are seen in the connection area of the inhibitors.

The dock results demonstrated that electrostatic largely contribute to the binding of inhibitors (Table 1). The MM/PB(GB)SA results also indicate that the electrostatic components (ΔE_{ele}+ΔG_{PB}) contribute more to the binding energy compared with the non-polar (ΔE_{vdw}+ΔG_{SA}) components. The larger difference between the dock scores and MM/PB(GB)SA results may be attributed to the fact the dock algorithm does not consider the contribution from the salvation and also the protein is kept fixed during the calculations.

The potency of the inhibitors is mainly governed by the π-π stacking interactions, hydrophobic interactions, and the van der Waals contacts of the inhibitors with the Arg24, Arg257, Met258, Arg254, and Phe182 in addition to the hydrogen bonding interactions. Calculated thermodynamic parameters for the complexation of the Sanggenon derivatives by MM/PBSA method analysis are shown in Table2.

The correlation between the information in this projection and the decomposition analysis acquired from the calculation of MM/GBSA is clear (Table 4). This compound binds to the PTP1B active site predominantly by both hydrophobic interactions and hydrogen bond binding interactions.

Conclusion

Molecular dynamics (MD) simulations for a period of 10 ns on complexed PTP1B had been fulfilled with the goal of disclosing the possible mechanisms of ligand recognition and inhibition. The maximum exceptional reality is the motion of the second one energetic site, and the sorts of interactions with it. According to our calculated van der Waals and electrostatic energies among PTP1B and the inhibitor Sanggenon, it is obtrusive that the greater contributions to the Van der Waals to PTP1B-inhibitor complexes conformation, binding site, the extra electrostatic interaction results, which is constant with

other to be had experimental research. By analyzing the interactions between PTP1B and the high-affinity inhibitor compound 1, it become observed that the residues adjoining to the second one active site, inclusive of, Met258, Arg24, Asp29, Arg254, and, might be partly accountable for the excessive inhibitory activity and selectivity of PTP1B. The MM/PBSA and MM/GBSA techniques produce similar binding energies and hence they each can be applied to calculated the binding energies for similar structures. In step with the MD simulations, MM/PBSA unfastened electricity calculations, and MM/GBSA free power decomposition analyses, we will make the subsequent conclusions. The simulation effects imply that PTP1B may be effective and selective inhibitors, which now not noted inside the literature, of Sanggenon molecule.

In the designing of extra effective medicine the development of such molecules and targeting the floor residues, as an example, the region containing Met258, Arg254, Gln102 and Asp29 of the second phosphate binding site is probably advantageous.

Primarily based on our dynamics simulation and decomposition evaluation, many beneficial outcomes were obtained. These could be employed to increase and layout new capsules.

Declarations

Acknowledgement

I would like to thank to DUBAP for their financial support (Project No: 10-FF-162), the numerical calculations reported in this paper were performed at TUBITAK ULAKBIM, High Performance and Grid Computing Center (TR-Grid e-Infrastructure) The Scientific and Technological Research Council of Turkey (TUBITAK).

Author contribution All authors equally contributed to this manuscript.

Code availability The calculations have been carried out using AMBER 11

provided by AMBER Software Company, Dock 6.0 have been used publicly available source code which are freely available on the internet.

Declarations

Conflict of interest The authors declare no competing interests.

Data availability We confirm the availability of all the data and materials in this manuscript.

References

1. SarathKumar, B, Lakshmi, BS (2019) In silico investigations on the binding efficacy and allosteric mechanism of six different natural product compounds towards PTP1B inhibition through docking

and molecular dynamics simulations. J Mol Model 25:272. https://doi.org/10.1007/s00894-019-4172-7

2. Chernoff J, Schievella AR, Jost CA, Erikson RL, Neel BG (1990) Cloning of a cDNA for a major human protein– tyrosine– phosphatase. Proc Natl Acad Sci 87:2735– 2739.
3. Shinde RN, Sobhia ME (2013) Binding and discerning interactions of PTP1B allosteric inhibitors: novel insights from molecular dynamics simulations. J Mol Graph Model 45:98–110.
4. Gu F, Dube N, Kim JW, Cheng A, Ibarra-Sanchez MJ, Tremblay ML, Boisclair YR (2003) Protein tyrosine phosphatase 1B attenuates growth hormone-mediated JAK2-STAT signaling. Mol Cell Biol 753– 3762.
5. Dube N, Tremblay ML (2004) Beyond the metabolic function of PTP1B. Cell Cycle 550– 553.
6. Bjorge JD, Pang A, Fujita DJ (2000) Identification of PTP1B as the major tyrosine phosphatase activity capable of dephosphorylating and activating c-Src in several human breast cancer cell lines. J Biol Chem 41439- 41446.
7. Byon, JC, Kusari, AB, Kusari (1998) J Protein-tyrosine phosphatase-1B acts as a negative regulator of insulin signal transduction. Mol Cell Biochem182:101–108 https://doi.org/10.1023/A:1006868409841
8. Jr Burke TR, Kole HK, Roller PP (1994) Potent inhibition of insulin receptor dephosphorylation by a hexamer peptide containing the phosphotyrosyl mimetic F2Pmp. Biochem Biophys Res Commun 129-134.
9. Montserat J, Chen L, Lawrence DS, Zhang ZY (1996) Potent low molecular weight substrates for protein-tyrosine phosphatase, J Biol Chem 271:7868-7872.
10. Rollinger JM, Spitaler R, Menz M, Marschall K, Zelger R, Ellmerer E P, Schneider P, Stuppner H (2006) Venturia inaequalis-Inhibiting Diels-Alder Adducts from Morus Root Bark J Agric Food Chem 8432-8436.
11. Cui L, Na M, Oh H, Bae E Y, Jeong D G, Ryu S E, Kim S, Kim BY, Oh WK, Ahn JS (2006) Protein tyrosine phosphatase 1B inhibitors from Morus root bark. Bioorg Med Chem Lett 1426–1429.
12. Lang PT, Moustakas D, Brozell S, Carrascal N, Mukherjee S, Pegg S, Raha K, Shivakumar D, Rizzo R., Case D, Shoichet B, Kuntz I (2007) University of California San Francisco, http://dock.compbio.ucsf.edu/
13. Case DA, Darden TA, Cheatham III TE, CL Simmerling, Wang J, Duke RE, Luo R, Walker RC, Zhang W, Merz KM, Roberts BP, Wang B, Hayik S, Roitberg A, Seabra G, Kolossvary I, Wong KF, Paesani F, Vanicek J, Liu J, Wu X, Brozell SR, Steinbrecher T, Gohlke, Cai Q, Ye X, Wang J, Hsieh M J, Cui G, Roe DR, DH. Mathews, M. G. Seetin, Sagui CH, Babin V, Luchko T, Gusarov S, Kovalenko A, Kollman PA (2010) AMBER 11, University of California: San Francisco.
14. Duan Y, Wu C, Chowdhury S, Lee M C, Xiong GM., Zhang W, Yang R, Cieplak P, Luo R, Lee T, Caldwell J, Wang MJ, Kollman P (2003) Point-charge force field for molecular mechanics simulations of proteins based on condensed-phase quantum mechanical calculations. J Comput Chem 1999-2012.

15. Case DA, Cheatham TE, Darden T, Gohlke H, Luo R, Merz KM, Onufriev A, Simmerling C, Wang B, Woods R J (2005) The Amber biomolecular simulation programs. J Comput Chem 1668-1688.
16. Deora GS, Karthikeyan C, Moorthy NS, V Rathore, AK Rawat, AK Tamrakar, AK Srivastava, P Trivedi (2013) Design, synthesis and biological evaluation of novel arylidine-malononitrile derivatives as non-carboxylic inhibitors of protein tyrosine phosphatase 1B Med Chem Res 5343-5348.
17. 17. Puius YA, Zhao Y, Sullivan M, Lawrence DS, Almo SC , Zhang ZY (1997) Identification of a second aryl phosphate-binding site in protein-tyrosine phosphatase 1B: A paradigm for inhibitor design. Proc Natl Acad Sci USA 13420–13425.
18. Pettersen EF, Goddard TD, CC Huang, Couch GS, Greenblatt DM, Meng EC, Ferrin TE (2004) UCSF Chimera—A visualization system for exploratory research and analysis J Comput Chem 1605-1612.
19. Accelrys Software Inc (2012) Discovery Studio Modeling Environment, Release 3.5, San Diego: Accelrys Software Inc
20. Turner PJ (2005) XMGRACE, version 5. Center for Coastal and Land-Margin Research, Oregon Graduate Institute of Science and Technology, Beaverton, Oregon;. http://plasma-gate.weizmann.ac.il/Grace/
21. Bayly CI, Cieplak P, Cornell WD, Kollman PA (1993) A Well- Behaved Electrostatic Potential Based Method Using Charge Restraints for Deriving Atomic Charges - the Resp Model. J Phys Chem 10269-10280.
22. Darden T, York D, Pedersen L (1993) Particle Mesh Ewald -and.Log(N) Method for Ewald Sums in Large Systems J Chem Phys 10089-10092.
23. Holger G, David AC (2004) Converging free energy estimates: MM-PB (GB)SA studies on the protein-protein complex Ras-Raf. J Comput Chem 25(2):238-50. DOI: 10.1002/jcc.10379
24. Hartshorn MJ, Murray CW, Cleasby A, Frederickson M, Tickle I J, Jhoti H (2005) Fragment-based lead discovery using X-ray crystallography. J Med Chem 403-413.
25. Weis A, Katebzadeh K, Söderhjelm P, Nilsson I, Ryde U (2006) Ligand affinities predicted with the MM/PBSA method: dependence on the simulation method and the force field. J Med Chem 6596-6606.
26. Gohlke H, Kiel C, Case DA (2003) Insights into protein-protein binding by binding free energy calculation and free energy decomposition for the Ras-Raf and Ras-RalGDS complexes J Mol Biol 891-913.

Figures

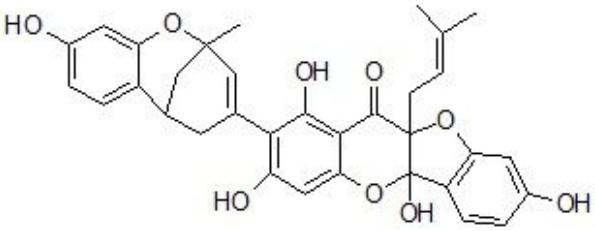

1: Sanggenon B

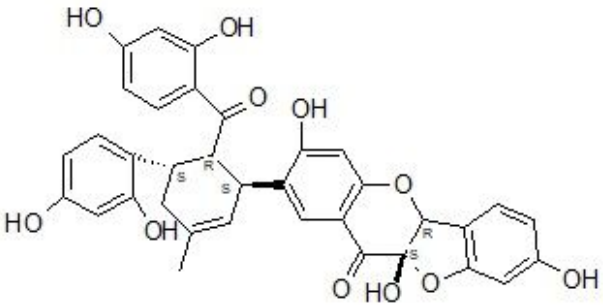

2: Sanggenon C

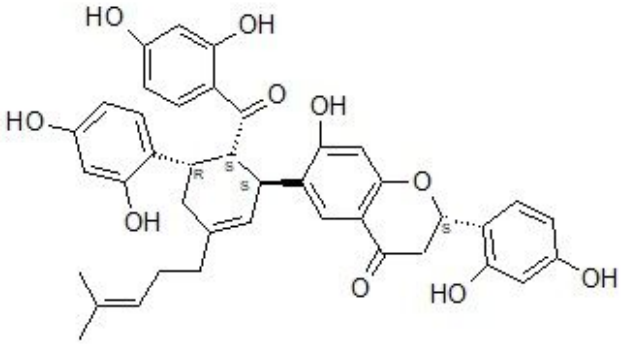

3: Sanggenon G

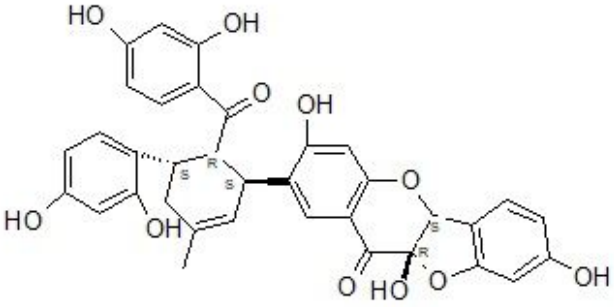

4: Sanggenon O

Figure 1

The 2-D structures Sanggenon derivative inhibitors.

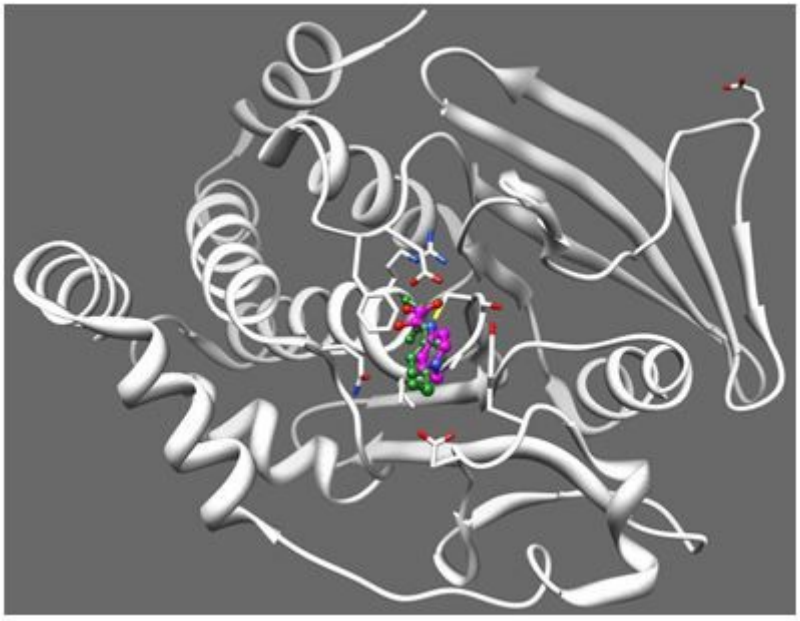

Figure 2

X-ray crystal structure of inhibitor 1 bound to PTP1B, re-dock the lead compound in X-Ray criystallography in to the protein domain, RMSD compared with criystallographic structure is 1.28 Å.

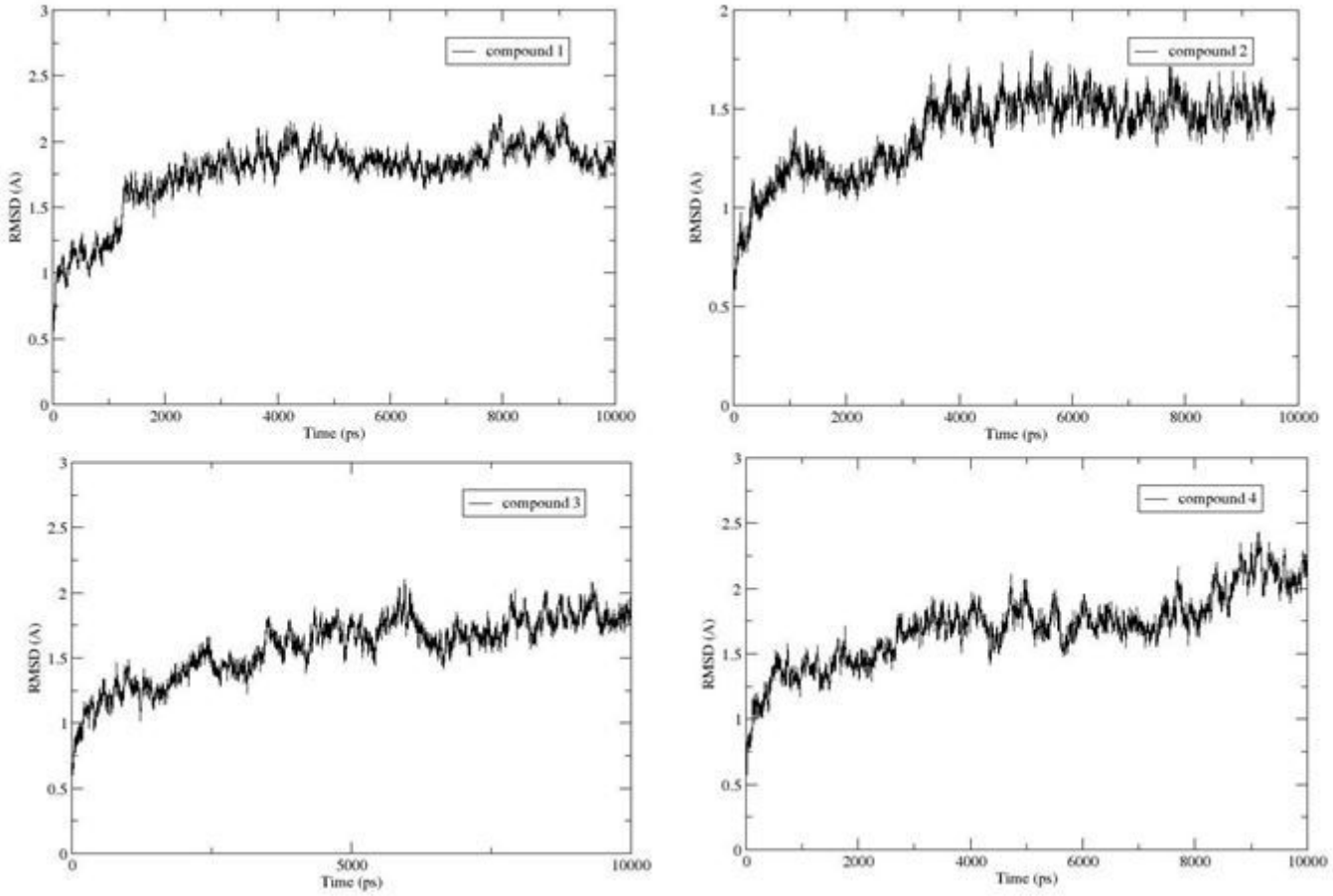

Figure 3

Root-mean square deviations (RMSD) of the backbone atoms (CA, N, C) of the complexes with respect to the first snapshot as a function of time.

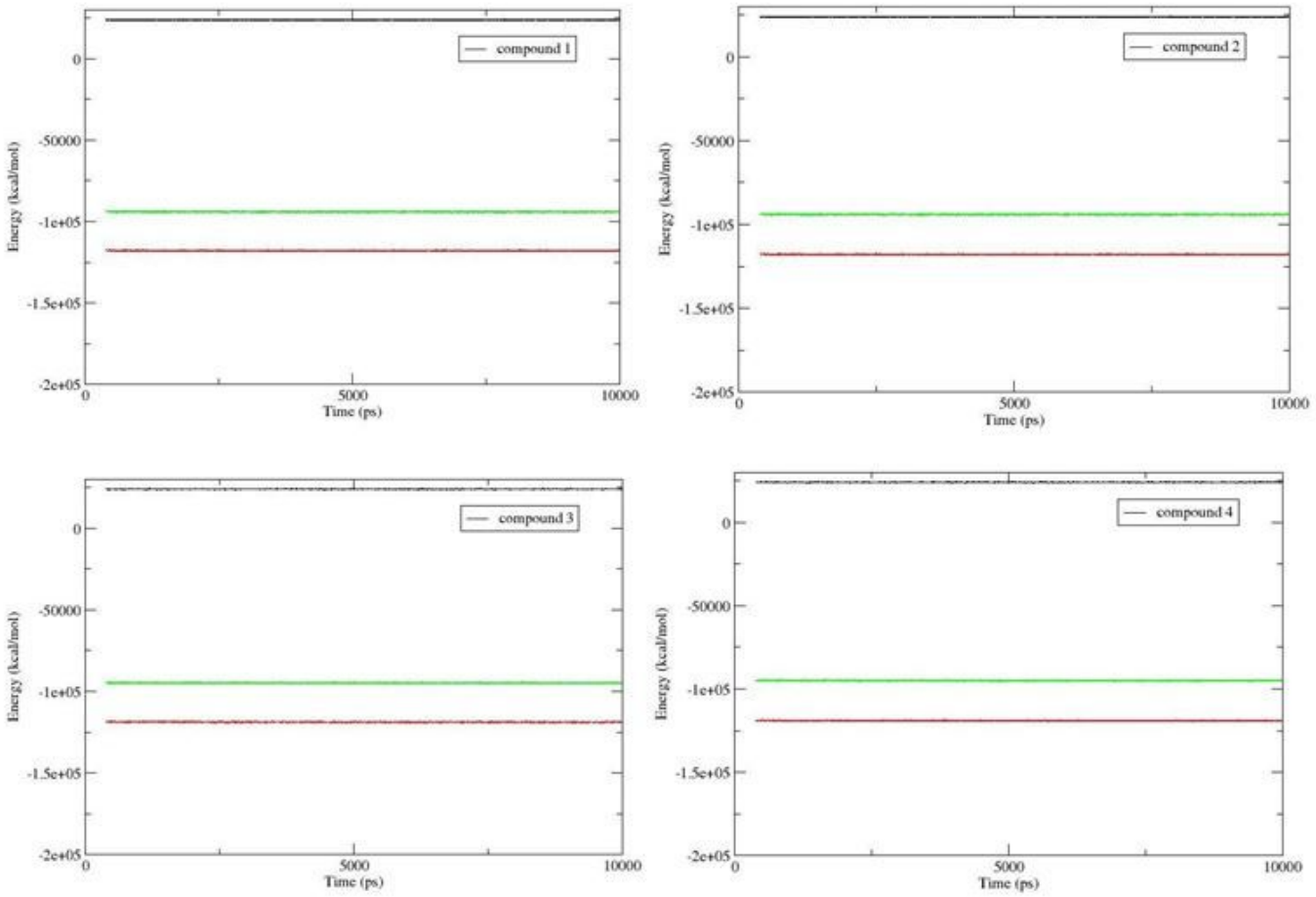

Figure 4

Black line represents kinetic energy, Green line represents total energy and red line represents potential energy.

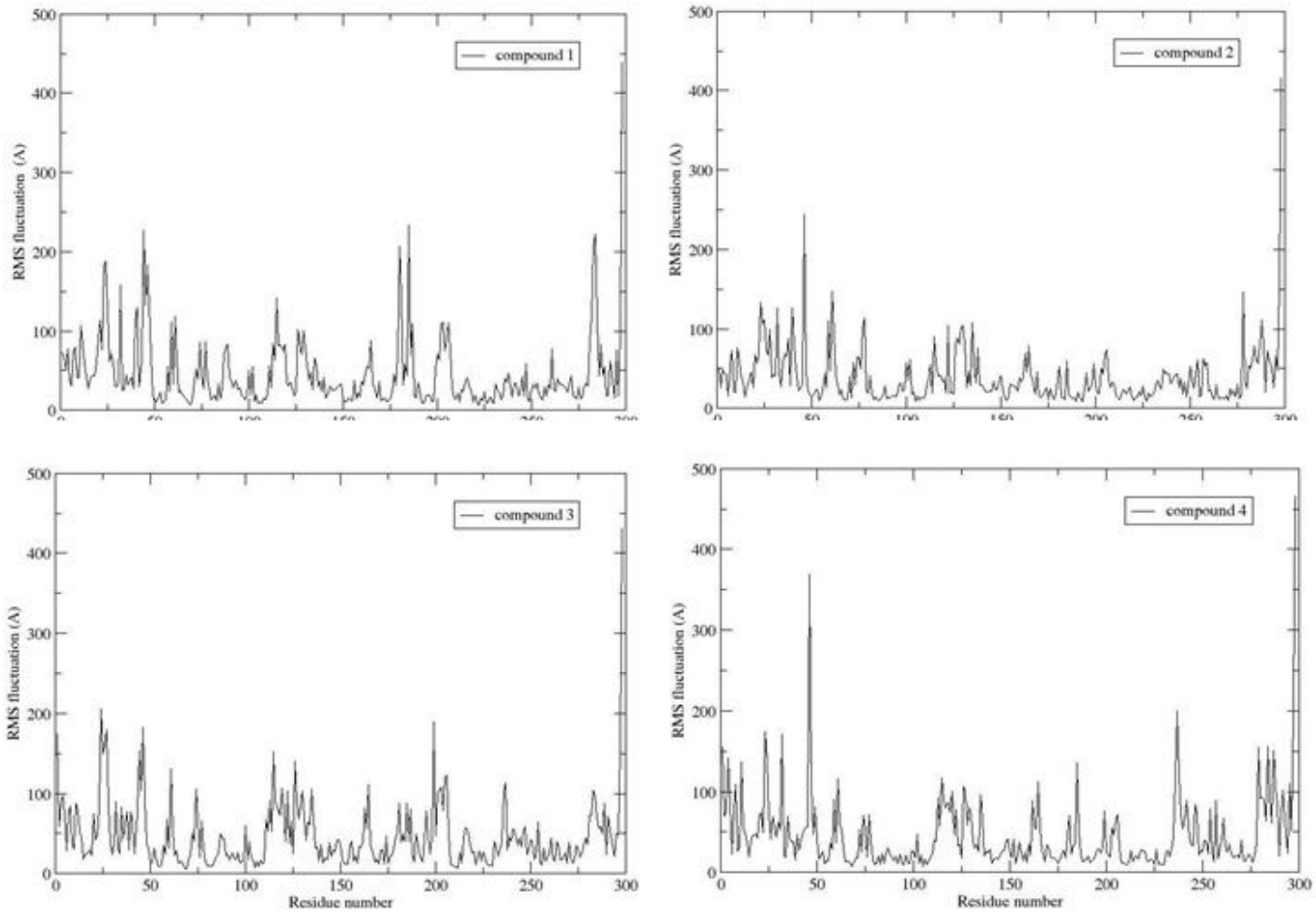

Figure 5

Root-mean square fluctuations (RMSF) of the backbone atoms (CA, N, C) versus residue number for (1-4 inhibitors) the PTP1B complex.

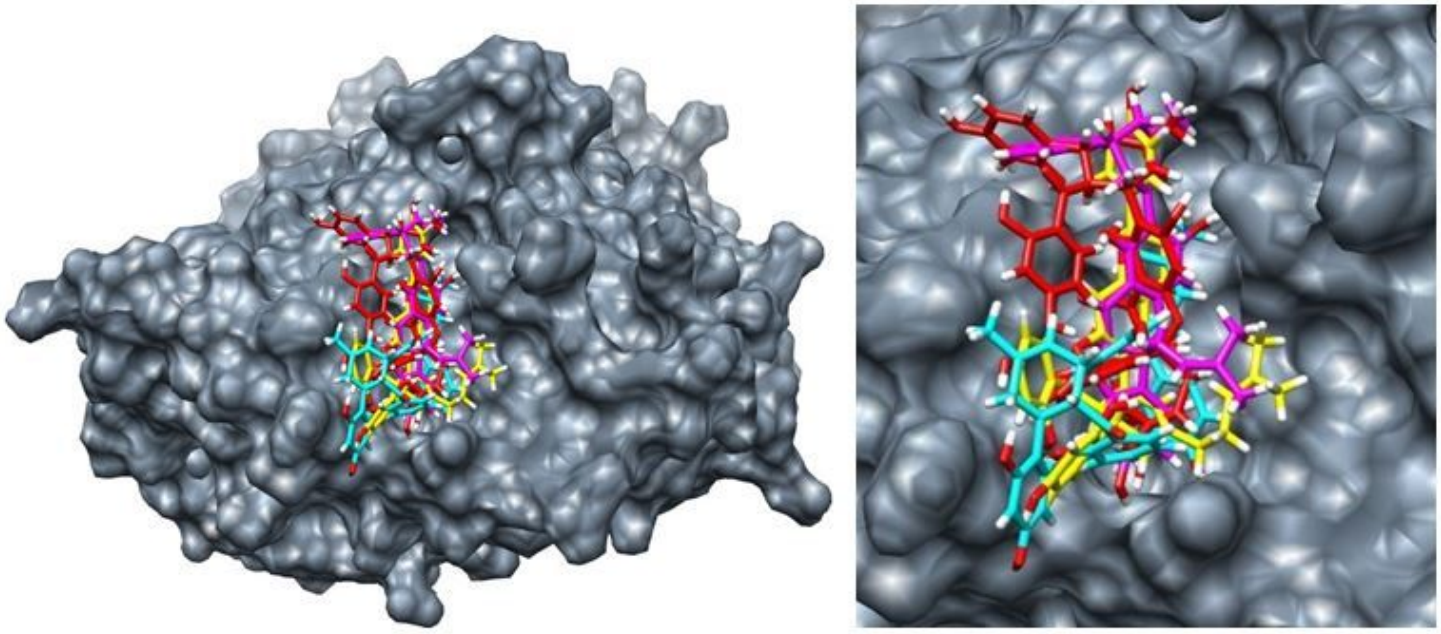

Figure 6

The structures were superimposed on the PTP1B for the comparison of the binding mode. Ligand 1 is colored in pink, Ligand 2 is in Cyan, Ligand 3 is in yellow and Ligand 4 is in red, respectively.

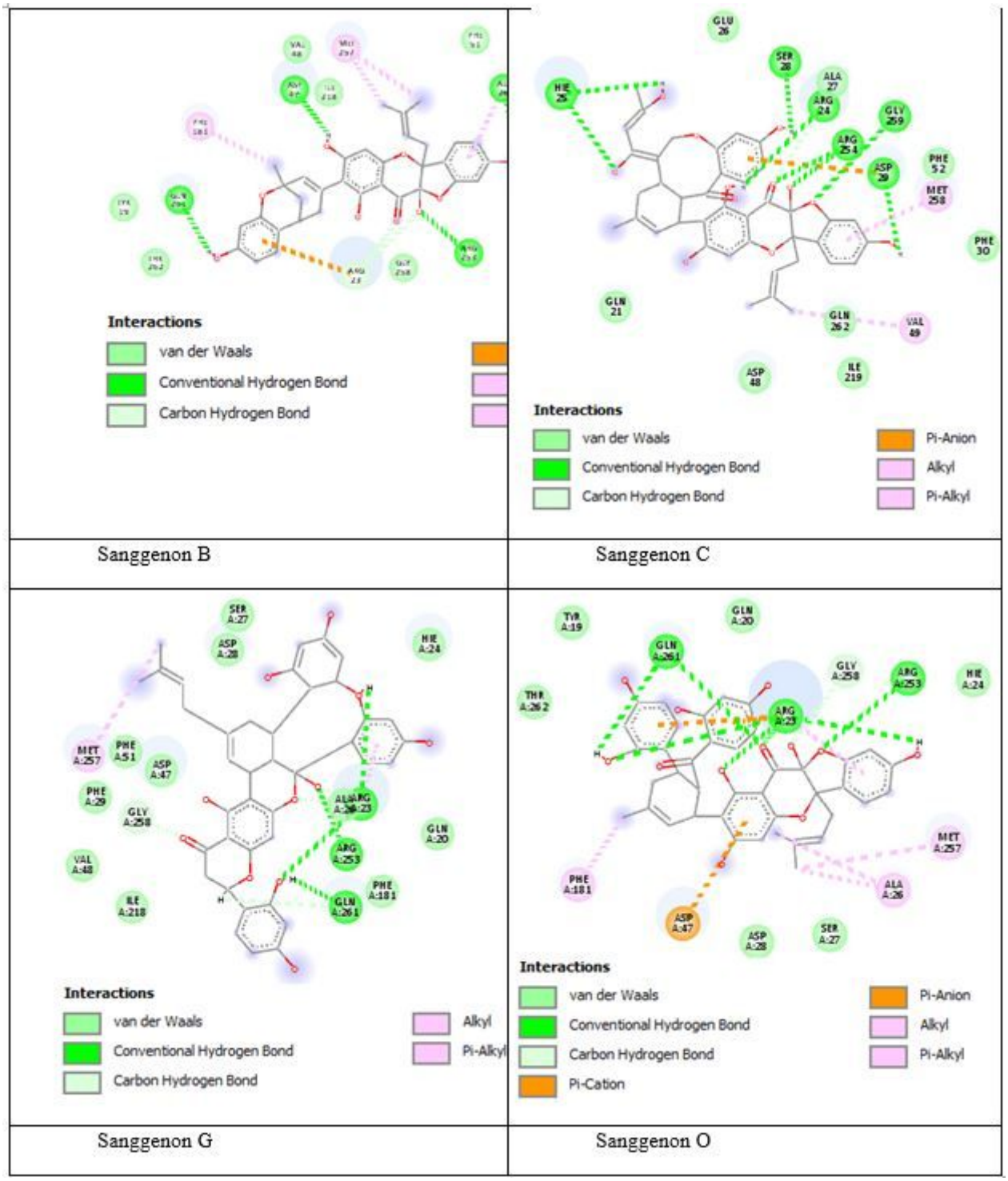

Figure 7

The two-dimensional diagram of the molecular docking. a The docking interactive model of PTP1B protein receptor with compound 1, compound 2 , compound 3 and compound 4.

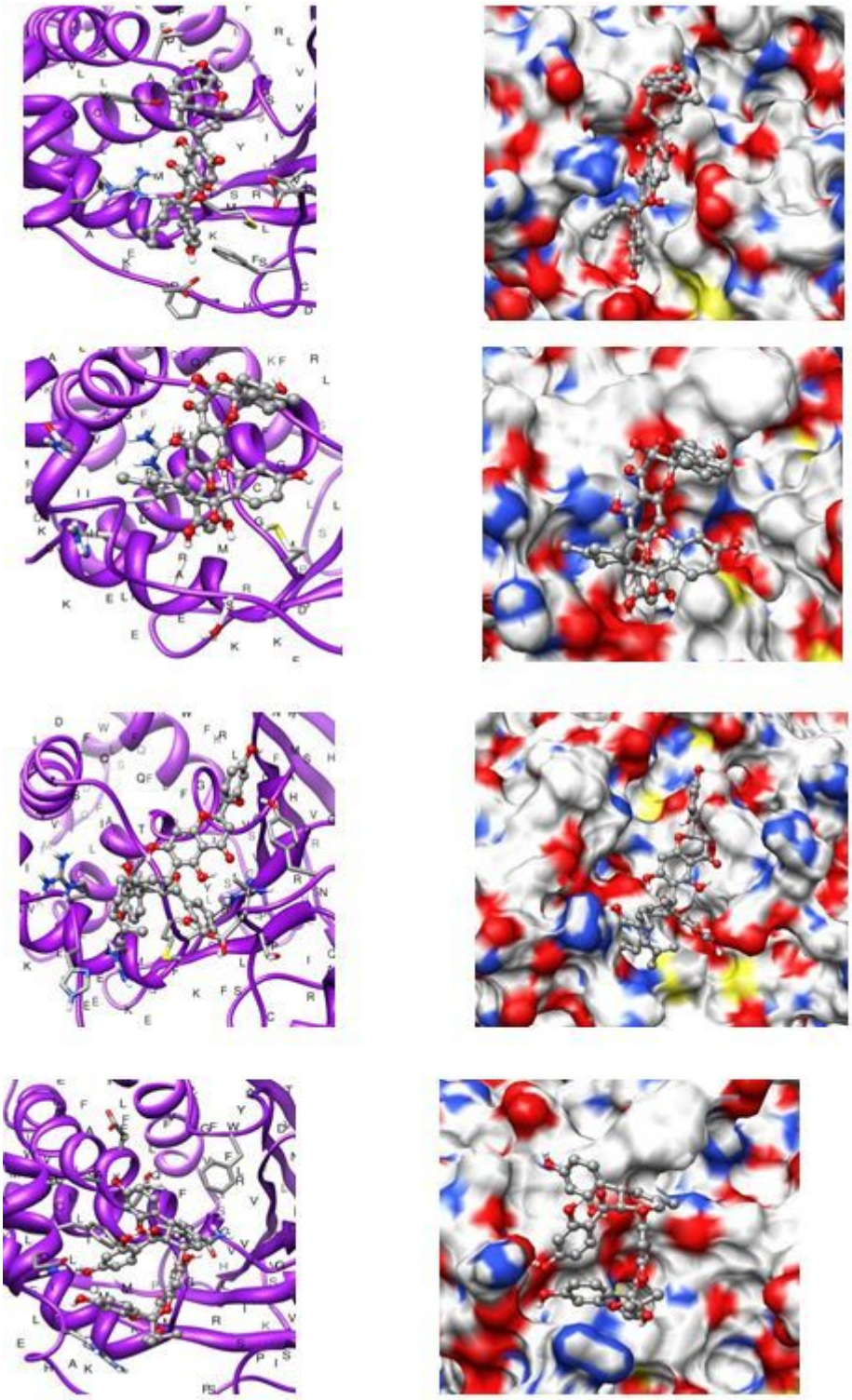

Figure 8

The orientation of the residues shown as sticks around inhibitor compounds in the final snophot of MD simulation.